

Conversion of Electrostatic to Electromagnetic Waves by Superluminous Ionization Fronts

D. Hashimshony and A. Zigler

Racah Institute of Physics, Hebrew University, Jerusalem, Israel

K. Papadopoulos*

Advanced Power Technology, Inc., Washington, D.C.

(Received 11 August 2000)

The conversion of static electric fields to electromagnetic radiation by the incidence of a superluminous ionization front on plasma is investigated. For extremely superluminous fronts, the radiation is close to the plasma frequency and is converted with efficiency of order unity. A proof-of-principle experiment was conducted using semiconductor plasma containing an alternately charged capacitor array. The process has important implications in astrophysical plasmas, such as supernova emission, and to laboratory development of compact, coherent, tunable radiation sources in the THz range.

DOI: 10.1103/PhysRevLett.86.2806

PACS numbers: 52.35.-g

Efficient conversion of electrostatic (es) plasma waves to electromagnetic (em) near the plasma frequency is a basic plasma physics problem with relevance to astrophysics [1,2]. The conversion is due either to breakdown of geometric optics in the presence of a sharp index of refraction gradients, especially near boundaries, or due to nonlinear interaction of electrostatic plasma waves with ion or electron density fluctuations. As discussed in several reviews [1,2], the conversion efficiency of these processes is very small. An often quoted process, by which em wave frequencies can be up-shifted, relies on reflection of an em wave (ω_o, k_o) incident upon an over-dense ($\omega_o \ll \omega_e$) plasma front moving with relativistic speed U . In this case, the leftward (reflected) wave will have a frequency ω_r given by the well-known double Doppler shift,

$$\omega_r/\omega_o = (1 + \beta_o)/(1 - \beta_o), \quad \beta_o = U/c. \quad (1)$$

The rightward (transmitted) wave will be evanescent confined within a skin depth behind the front.

It was noted more than 20 years ago [3–6] that reflection can occur not only from a moving plasma but also from a moving over-dense plasma boundary, such as an ionization or recombination front. Lampe *et al.* [6] studied the interaction of an em wave with an over-dense ionization front moving with superluminous speed. Such fronts often occur in astrophysical plasmas due to UV ionization. They noted that reflection cannot occur from such a front, since a reflected pulse will be overrun by the front. Instead, the interaction results in two “transmitted” waves that, in the laboratory frame, are moving in the direction of the front. Sorokin and Stepanov [3] found that an ionization front, moving with a uniform velocity U in a dielectric with permittivity ε , behaves as a drifting plasma layer with equivalent dielectric constant given by

$$\varepsilon(\omega) = \varepsilon\{1 - [\omega_e^2/\omega(\omega - i\gamma)](1 - \beta)(1 + \beta)^{-1}\}. \quad (2)$$

In Eq. (2), $\beta = (U/c)\sqrt{\varepsilon}$, and γ is the wave dephasing factor. The dispersion relation for em waves in the system is then given by

$$(kc/\omega)^2 = \varepsilon(\omega). \quad (3)$$

For $\beta \ll 1$, we recover the usual plasma dielectric function that results in reflection by an over-dense front. However, for superluminous speeds ($\beta > 1$), neither wave has a cutoff, since $\varepsilon(\omega) > 0$ at any frequency. Both the right and the left wave are transmitted propagating waves. Since a moving ionization front represents a discontinuity in both space and time, both ω and k for the transmitted waves are different from the incident wave. Evaluation of the frequencies and power transferred from the incident wave to the transmitted waves is greatly simplified if we assume a sharp discontinuous front (in the scale of the incident wavelength). In this case, it is sufficient to complement Eqs. (2) and (3) with the continuity boundary conditions at the front. These can be met only if all waves are in phase at the front, i.e.,

$$-k_o Ut - \omega_o t = -kUt - \omega t. \quad (4)$$

Solving Eqs. (2)–(4), we find that the frequencies of the two transmitted waves are given by [6]

$$\omega/\omega_o = [1 \pm \beta\sqrt{\varepsilon(\omega_o)}]/(1 - \beta). \quad (5)$$

In the limit of $\beta \gg 1$, the transmitted frequencies and wave numbers are

$$\begin{aligned} \omega_{1,2} &= \mp \omega_o [1 + (\omega_e/\omega_o)^2]^{1/2}, \\ k_{1,2} &= \pm (\omega_{1,2}/c) [1 - (\omega_e/\omega_{1,2})^2]^{1/2}. \end{aligned} \quad (6)$$

From Eqs. (6), we can see the following in the limit of large β : (i) Both ω and k are real; (ii) both transmitted waves propagate in the direction of, but slower than, the

front; (iii) for values of $\omega_o \ll \omega_e$, the frequency of the observed radiation in both modes approaches the plasma frequency.

The amplitude of the reflected waves can be found for an arbitrary profile of the front using the formal technique of the ‘‘auxiliary reflection front’’ first presented by Stepanov [3]. For a sharp, step function front, it suffices to apply the boundary conditions on the discontinuity surface; these conditions require that the tangential parts of E and B are continuous [6] across the front. For $\beta > 1$, we find that

$$\begin{aligned} E_1/E &= [1 + \sqrt{\varepsilon(\omega_0)}]/2\sqrt{\varepsilon(\omega_0)}, \\ E_2/E &= [\sqrt{\varepsilon(\omega_0)} - 1]/2\sqrt{\varepsilon(\omega_0)}. \end{aligned} \quad (7)$$

Notice that, for $\beta \gg 1$ and $\omega_o \ll \omega_e$, both reflection coefficients become $\frac{1}{2}$. A peculiarity in this case is that the total energy in the secondary waves is smaller than that of the primary wave. This is a well-known effect [3–6] and it can be attributed to the excitation of a zero frequency pure ‘‘magnetic wave’’ in the plasma with wave number k_0 . The magnetic wave is formed because, when the electrons are suddenly created, they are accelerated by the electric field of the em wave with a phase such as to create the static magnetic field. These considerations indicate that approximately half the energy is stored and eventually dissipated in the medium, while the rest is radiated at the up-shifted frequencies.

The above analysis has been performed assuming a plane infinitely long em wave. It is easy to see that, for a finite length pulse, the number of cycles N will be preserved in the secondary waves. Most importantly, the theory can be trivially extended to the conversion of energy stored in es waves in a weakly ionized medium, if the conditions $\omega_o \ll \omega_e$ and $k_o \ll c/\omega_e$, where ω_e is the plasma frequency following ionization, are satisfied. After all, in the limit of long wavelengths ($k_o \cong 0$, i.e., dipole approximation) the es and em wave fields are indistinguishable. This has profound implications to astrophysics, since it provides a mechanism to convert energy stored in low frequency es or em turbulence to high frequency propagating em waves with efficiency of the order unity. Furthermore, it can provide a tunable device for generating efficiently em waves in spectral regions where efficient sources are not available.

Aspects of the above theory have been experimentally verified only for the subluminescent case [7–10]. In particular, Savage *et al.* [7] experimentally demonstrated up-shifting of incident radiation from laser generated ionization fronts in a gas. Furthermore, Lai *et al.* [8] and Muggli *et al.* [9] demonstrated the extension of the theory to conversion of es waves by a subluminescent ionization front. In their particular experiments, the electrostatic field was formed by an alternately biased capacitor array placed in a neutral gas photoionized by a laser front propagating subluminescently. They confirmed the theoretical

result that the radiating frequency depends only on the wavelength k_o and the front speed U and is given by

$$\omega = k_o U/2 + \omega_e^2 2k_o U. \quad (8)$$

Equation (6), on the other hand, valid for $\beta \gg 1$, indicates that, for $\omega_o \ll \omega_e$ to zero order, the emitted radiation is near ω_e independently of the wavelength of the static wave and of the value of β . This theoretical prediction has important implications to the generation of coherent radiation in both astrophysical and laboratory settings.

We present below a proof-of-principle experiment of conversion of low frequency es waves to em waves at the plasma frequency using a superluminescent ionization front. Most importantly for astrophysical applications, the paper presents the first experimental demonstration that, for highly superluminescent speeds, $\beta \gg 1$, the emitted frequency coincides with the plasma frequency of the front. Furthermore, it is essentially independent of the speed of the front, and of the details of the electrostatic turbulence converted to em waves.

In the experiment, the low frequency es turbulence was modeled by using the static field of an alternating biased capacitor array similar to the one used in the subluminescent case [7,8]. However, in contrast to the subluminescent experiments, performed in a gaseous medium, our experiments used a semiconductor crystal. There are several reasons for using a semiconductor. First, since $\varepsilon \gg 1$, it is relatively easy to satisfy the condition $\beta \gg 1$ while preserving long interaction paths. Second, the photoionization energy is much smaller than for a gas. Third, the system is much easier to handle and diagnose.

The experimental setup is shown in Fig. 1. It consists of the following: a mode locked Ti:sapphire 100 fs laser, operating at 0.8 μm wavelength, with maximum energy per pulse of 2 mJ and repetition rate 10 Hz; a beam splitter that divides the laser beam into two; a zinc selenide (ZnSe) crystal with $\varepsilon \sim 9$ placed between two thin glass plates with a multiple electrode structure alternately biased; focusing and collimating optics; an optically gated detector; a variable delay line that gates the detector with respect to the emitter; a current amplifier; and a fast current sampler connected to a low-noise current amplifier and a boxcar integrator.

The measurement system of the experiment is a ‘‘pump and probe’’ system similar to the one used by Jeon *et al.* [11]. The electrically biased ZnSe radiating structure was cut and polished to the specific shape. A static periodic waveform was created with a multiple (3×10 mm) electrode structure made by evaporation of Al on two thin glass plates separated by 3 mm. ZnSe is a direct band gap crystal with 2.7 eV excitation energy. Therefore, the carrier generation involves two photons, and the absorption depth δ depends on the intensity I of the laser. It is given by $\delta = 1/\alpha I$, where α is the two-photon absorption coefficient. This allows much deeper, as well as controlled, penetration of the laser

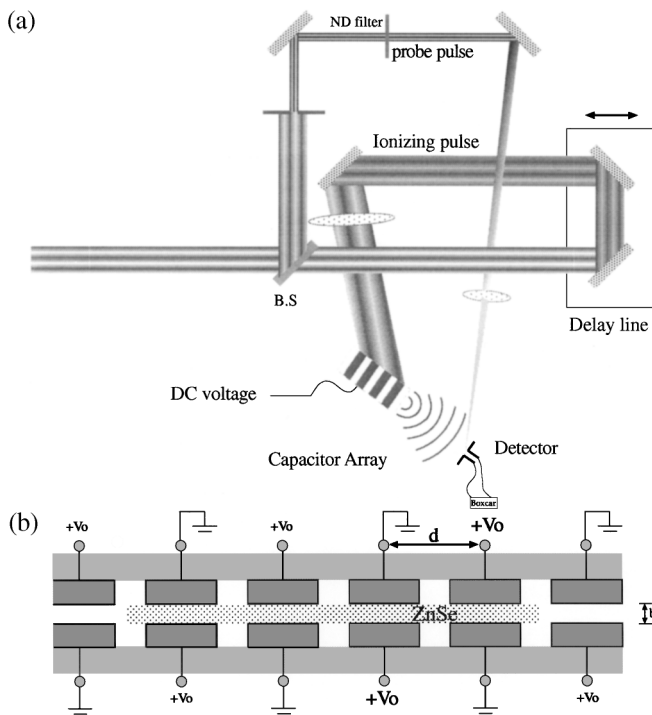


FIG. 1. (a) Experimental setup. (b) Capacitor array.

radiation. In our experiments, the penetration depth was chosen so that it satisfied the condition $\delta \gg c/\omega_e$. This condition is a necessary one for the plasma to support bulk rather than surface plasma waves. Notice that for single photon absorption $\delta \ll c/\omega_e$ and only surface waves will be excited.

The electromagnetic radiation was generated by sweeping the 100 fs laser pulse at an oblique angle of incidence to the crystal. The laser beam was split into two beams. The main beam carrying more than 90% of the energy served as the pump beam, and the second beam served as the probe beam. The main beam was focused by a cylindrical lens on the side of the crystal to form the propagating ionizing front. The crystal was placed at a 20 degree angle to the pump laser beam front. A gated planar dipole antenna monitored the amplitude of the radiated electric field. The antenna detector was gated at different delay times by varying the optical delay between the pump and the probe laser pulses. The maximum frequency response of the configuration was approximately 2 THz, dictated by the carrier lifetime of <0.5 ps. The amplitude of the induced, time dependent voltage across the gap was determined by measuring the average current driven in the antenna circuit during the laser probe beam irradiation. An SRS250 boxcar integrator was used to collect these short current pulses. The current was averaged over 10000 pulses for each delay stop. The profile of the radiation electric field was determined by monitoring this average current vs the time delay between the pump laser beam and the probe laser beam. The value of the detected current was transferred to the computer, together with the position of the

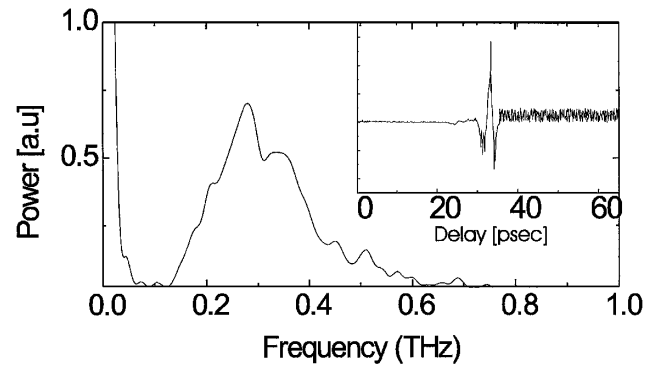


FIG. 2. The radiation spectrum. The inset shows temporal scan of the electric field vs delay time.

optical delay line monitored by the encoder. A full scan contained about 120 delay points. The repetition rate was limited by the laser system only.

A set of experiments was performed using a single capacitor ($N = 1$) and varying the laser fluence. A typical temporal scan of the emitted radiation electric field is shown in the inset of Fig. 2. The scan represents the measured field amplitude vs the delay between the pump and the probe laser pulse for $W = 0.3$ mJ. The scan length and step size were adjusted so that the full waveform could be recovered. Each scan was initiated long before the emitted radiation reached the detector and terminated upon reaching zero. This was done to ensure that the complete signal was scanned and recorded.

Figure 2 shows the radiation spectrum indicating a central emission frequency of 0.3 THz, which corresponds to a carrier density of 5×10^{14} cm $^{-3}$. The bandwidth is of the order of unity.

In our experiment $\beta^2 \epsilon \gg 1$. Thus, using Eq. (6) for $\omega_o = 0$, the radiation frequency scales as the square root of the carrier density n , $\omega \sim \sqrt{n}$. For two-photon absorption, the plasma density n , found by balancing the production rate with the recombination rate, will be given by

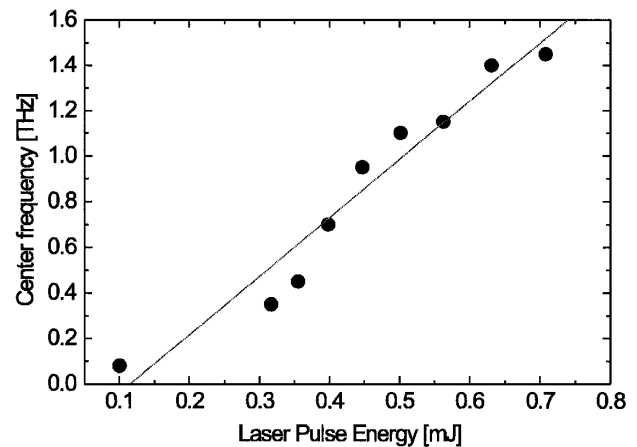


FIG. 3. Scaling of central radiation frequency with laser fluence.

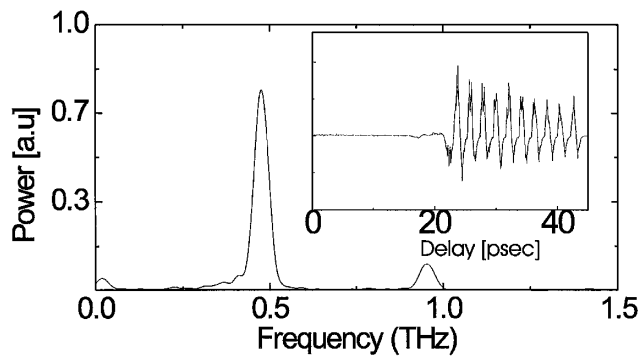


FIG. 4. Same as Fig. 2 but with $N = 10$ and $W = 0.35$ mJ.

$$n = \alpha W^2 / h\nu S^2 \tau. \quad (9)$$

In Eq. (9), W is the laser energy per pulse, ν and τ are the laser frequency and the pulse length, and S is the illuminated area of the crystal. From Eqs. (9), we find that, for $S = \text{constant}$, $\omega \sim W$. This scaling is confirmed in Fig. 3, which shows the central frequency of the recorded signal as a function of the laser fluence W in the range between 0.1 and 1 mJ.

A number of experiments were conducted to explore the effect of the spatial structure of the es wave on the spectrum. Figure 4 shows the temporal structure and spectrum for a periodic wave structure with $N = 10$ for $W = 0.35$ mJ. The output pulse is $N/2$ long, i.e., its time duration is N/ω , and its bandwidth scales as $\Delta\omega/\omega \approx 2/N$. This scaling is similar to the subluminescent case [7,8]. Notice that the central frequency is approximately 0.4 THz following the scaling shown in Fig. 3. Figure 5 shows the radiated waveform for a spatial spectrum of es waves with $N = 10$ but with capacitors 4 to 7 disconnected for $W = 0.3$ mJ. Notice that, while the central frequency is 0.3 THz, consistent with Fig. 4, the spatial static structure has been transformed into a temporal one.

In this Letter, we studied conversion of low frequency es fields to em waves by the interaction with a superluminescent ionization front. It was shown theoretically and confirmed experimentally that, for $\beta \gg 1$, the es fields are converted

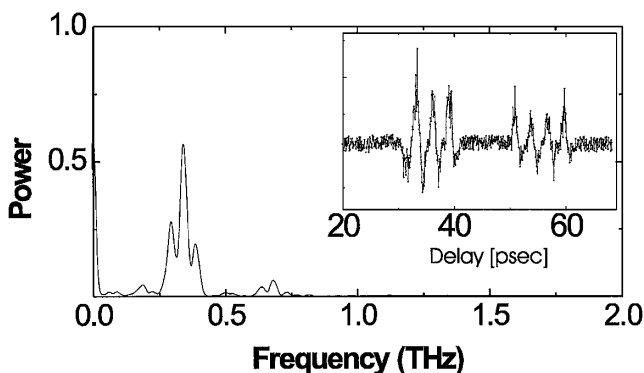


FIG. 5. Same as Fig. 4 but with capacitors 4–7 unbiased.

to em radiation at the plasma frequency of the front. Besides their intrinsic scientific interest, the results have important practical implications to the generation of radiation in the 0.3–10 THz range. Exploration of this region of the em spectrum has been frustrated by the lack of compact, efficient, tunable coherent sources of radiation. Recent developments in this area include the photoconductive (Austin) switch and large aperture photoconductive arrays [12]. These devices have a superficial resemblance to our setup in that they are using a femtosecond laser in conjunction with a biased semiconductor substrate, most often GaAs. However, the radiation process is simply a current surge (dJ/dt) that radiates while shorting the switch. The semiconductor acts as a conductor and does not support plasma modes. These operate on a regime in which the discharge time is longer than the dephasing time, lack temporal coherence, and cannot be tuned. Our process should also be distinguished from THz radiation observed in a number of recent experiments [13] of femtosecond laser pulses with heterostructures or n -doped GaAs. In this case, the radiation is very weak and is attributed to conversion at the boundaries of coherent space charge electron-hole plasma oscillations in the ballistic transport regime. In these experiments, the absorption depth $\delta \ll c/\omega_e$. As a result, the plasma supported only es surface waves—surface plasmons. Their conversion to em waves is an extremely inefficient process.

*Permanent address: Physics Department, University of Maryland, College Park, MD 20742.

- [1] S. A. Kaplan and V. N. Tsytovich, *Sov. Phys. Usp.* **12**, 42 (1969).
- [2] K. Papadopoulos and H. P. Freund, *Space Sci. Rev.* **24**, 511 (1979).
- [3] Yu. M. Sorokin and N. S. Stepanov, *Sov. Phys. Radiophys.* **14**, 19 (1971).
- [4] L. A. Ostrovskii and N. S. Stepanov, *Sov. Phys. Radiophys.* **14**, 387 (1971).
- [5] V. I. Semenova, *Sov. Phys. Radiophys.* **10**, 599 (1967); **15**, 505 (1972); **15**, 1375 (1972).
- [6] M. Lampe, E. Ott, and J. H. Walker, *Phys. Fluids* **21**, 42 (1978).
- [7] R. L. Savage, R. P. Brogle, W. B. Mori, and C. Joshi, *IEEE Trans. Plasma Sci.* **21**, 5 (1993).
- [8] W. B. Mori, T. Katsouleas, J. M. Dawson, and C. H. Lai, *Phys. Rev. Lett.* **77**, 464 (1996).
- [9] P. Muggli, R. Liou, C. H. Lai, J. Hoffman, C. Joshi, and T. Katsouleas, *Phys. Plasmas* **5**, 2112 (1998).
- [10] E. Esarey, P. Sprangle, B. Hafizi, and P. Serafim, *Phys. Rev. B* **53**, 6419 (1996).
- [11] T. Jeon and D. Grischkowsky, *Appl. Phys. Lett.* **72**, 3032 (1998).
- [12] M. C. Nuss and J. Orenstein, in *Millimeter and Submillimeter Wave Spectroscopy of Solids*, edited by G. Gruner (Springer, New York, 1998), pp. 7–48.
- [13] W. Sha, A. Smirl, and W. F. Tseng, *Phys. Rev. Lett.* **74**, 4273 (1995).